

A RISK-BENEFIT ANALYSIS OF THE SEISMIC EARLY WARNING SYSTEM FOR HIGH-SPEED RAILWAYS

Makoto SHIMAMURA
Senior Chief Researcher
Safety Research Laboratory
East Japan Railway Company
2-10-1 Yurakucho, Chiyoda-ku, Tokyo
100-0006 Japan
Fax: +81-3-5219-8678
Email: m-shimamura@head.jreast.co.jp

Hisashi TSUYUKI
Researcher
Safety Research Laboratory
East Japan Railway Company
2-10-1 Yurakutcho, Chiyoda-ku, Tokyo
100-0006 Japan
Fax: +81-3-5219-8678
Email: tsuyuki@head.jreast.co.jp

Tadao UMEZAWA
Professor
Department of Civil Engineering
Tokyo University
7-3-1 Hongo, Bunkyo-ku, Tokyo
113-8656 Japan
Fax: +81-3-5841-7798
Email: umezawa@trip.t.u-tokyo.ac.jp

Nodoka UJITA
Research Associate
Department of Civil Engineering
Tokyo University
7-3-1 Hongo, Bunkyo-ku, Tokyo
113-8656 Japan
Fax: +81-3-5841-7798
Email: ujita@trip.t.u-tokyo.ac.jp

Abstract: One of the major protective features of Shinkansen, the Japanese high-speed railway system, against earthquakes is a Seismic Early Warning System which detects the occurrence of earthquakes before the strong ground motion reaches the line. This study addresses a formulated method to quantify the cost-benefit trade-offs between the gain in safety and the costs associated with false alarms under various alternative configurations of the system.

Key Words: risk analysis, cost-benefit analysis, seismic early warning, high-speed railways

1. INTRODUCTION

Since Japan sits atop the junction of the Pacific, Eurasian and Philippine tectonic plates, and has accordingly suffered the devastation of major earthquakes throughout its history, the seismic risk is an important consideration among the overall safety issues for the nationwide railway network, especially the Shinkansen system. For the protection of this transportation system against earthquake, a Seismic Early Warning System (SEWS) is being operated that automatically induces a train to stop when a potentially destructive earthquake is detected at an accelerometer which is located near the epicenter.

Alike many other warning systems, one of the major managerial concerns for the operator of SEWS is to find the optimal trade-off between gain in safety and the costs associated with false alarms issued by the system. In order to address this target, this study develops a procedure for seismic risk analysis tailored to the Tohoku Shinkansen focusing on the effectiveness of the existing SEWS and of alternatives to it.

The procedure includes the standard method of earthquake hazard analysis (identification of seismic sources, estimation of recurrence parameters and specification of attenuation model). It also includes the special features for the seismic risk analysis of railway systems such as the spatially distributed nature of the system, the seismic behavior of running trains and track structures, relationship among earthquake magnitudes, epicentral locations, the activation/non-activation patterns of the warning systems and the probability that a train at a given location derails.

2. THE CURRENT SEWS OF THE TOHOKU SHINKANSEN

The Tohoku Shinkansen is a high-speed railway along the eastern side of Honshu, the largest of the Japanese islands operated by East Japan Railway, one of the railway companies that

emerged from the privatization of the previous Japanese National Railways. The line is about 500 km long and links Tokyo to the northern city Morioka with 16 intermediate stations.

The structure of the line is comprised of continuous double-track viaducts, not of embankments as most conventional railway lines in Japan do, except for tunnels in mountainous parts of the line. Accelerometers are installed at 11 coastal seismic stations and 24 wayside seismic stations, each of which is corresponding to one of 24 non-overlapping operational track segments. The locations of coastal stations are chosen to provide the longest lead time for a train to stop safely for offshore earthquakes. Each coastal accelerometer controls a preset operational track segment as shown in Figure 1. Therefore, as the intensity of ground motion at a coastal station exceeds the chosen threshold level, emergency braking is automatically activated for all trains running in the corresponding track segment.

The wayside system consists of 24 accelerometers installed at nearly equal intervals between Tokyo and Morioka. They operate for protect against inland earthquakes and also as a second line of defense against offshore earthquakes that might not be triggered by the coastal stations. Furthermore, the intensity of ground motion recorded at a wayside station is the basis for operational decisions.

After an earthquake triggered emergency train braking, operational actions to be taken vary depending on the intensity of the ground motion recorded at a wayside station. Train operation is to be resumed as soon as the intensity of the ground motion at a wayside station is proved to be so small that there is obviously no need of post-earthquake track inspection. In this case, only a short delay, typically several minutes, will be caused to the train operation. Otherwise, a post-earthquake inspection will be made either quickly by on-board or more carefully by on foot depending on the intensity of the ground motion. These cases can cause longer delays to the train schedule, typically around a couple of hours in the former case and a several hours in the latter case.

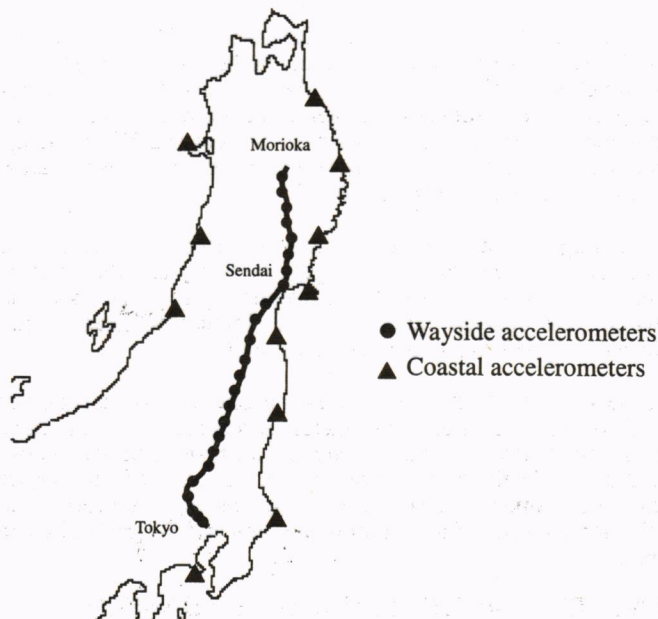


Figure 1: Tohoku Shinkansen line; location of stations and of wayside and coastal accelerometers

Both coastal and wayside stations can trigger emergency braking on Peak Ground Acceleration (PGA) of S waves and also on P wave information. The obvious advantage of using P waves is increase in lead time of emergency braking. This benefit is counterbalanced by increase in the rate of false alarms to some degree due to the limited accuracy of P wave based detection.

3. MODELING THE SYSTEM

Here we formulate a set of procedures to quantify the trade-off between safety and the rate of false alarms induced by various SEWS on the basis of previous risk studies[1],[2] and for the contemporary system settings of the Tohoku Shinkansen.

3.1 Seismic Environment

The earthquake activity in the region surrounding the Tohoku Shinkansen may be broadly divided into the Pacific Ocean seismicity, the inland seismicity and the Sea of Japan seismicity. This division can be observed in the map of earthquake epicenters, shown in Figure 2. The Pacific offshore earthquakes contribute 80 to 90 % of the earthquake occurrence rate in the area and are often of larger magnitude. However, these events occur at a distance of at least 80 to 100 km from the line and therefore subject to higher attenuation. These characteristics of the regional seismicity motivate the philosophy of the SEWS stated above.

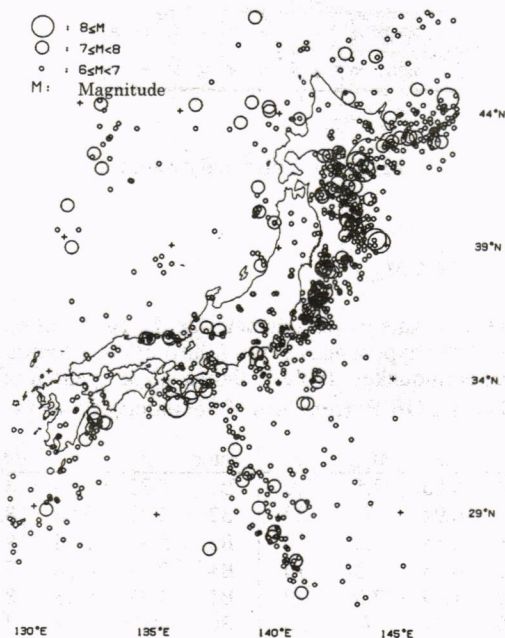


Figure 2: Historical Earthquake Epicenters in and around Japan

To model the seismic environment of the Tohoku Shinkansen, we have defined 20 seismicity sectors within which earthquake activity is considered uniform: see Figure 3. The areas and configuration of the seismic sectors were determined based on the distribution of the location and the magnitudes of historical earthquake. A statistical analysis of the historical data produces estimates of $\lambda(M)$, where $\lambda(M)$ is the rate in events/year of earthquakes of magnitude larger than M in a seismogenic source. We assume that $\lambda(M)$ follows the Gutenberg-Richter relationship:

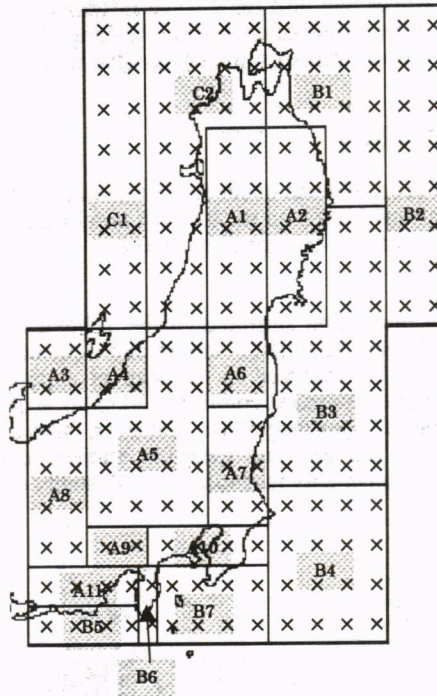


Figure 3: Seismicity Sectors

$$\log_{10} N(M) = a - bM, \quad M < M_{max} \tag{1}$$

where, a, b and M_{max} are constants which characterize the nature of each seismogenic source. Also the median values of the hypocentral depth h (km) of each source are estimated based on the database of historical earthquakes. Table 1. shows a, b, M_{max} and h of each sources.

Table 1:GR Parameters of Seismicity Sources

| sector | a | b | M_{max} | h | sector | a | b | M_{max} | h |
|--------|------|------|-----------|-----|--------|-------|------|-----------|-----|
| A1 | 3.04 | 0.86 | 7.5 | 10 | B1 | 5.85 | 1.13 | 8.5 | 40 |
| A2 | 3.81 | 0.94 | 7 | 30 | B2 | 3.79 | 0.85 | 8.5 | 20 |
| A3 | 1.15 | 0.65 | 7.8 | 10 | B3 | 5.98 | 1.14 | 8.5 | 20 |
| A4 | 2.29 | 0.75 | 7.8 | 10 | B4 | 2.25 | 0.68 | 7.5 | 20 |
| A5 | 4.33 | 1.09 | 7.5 | 20 | B5 | 1.37 | 0.53 | 8.6 | 20 |
| A6 | 4.95 | 1.11 | 7 | 20 | B6 | -0.02 | 0.34 | 7.5 | 10 |
| A7 | 4.34 | 0.96 | 7.2 | 50 | B7 | 8.92 | 1.68 | 8.2 | 10 |
| A8 | 2.73 | 0.76 | 8.1 | 10 | C1 | 4.85 | 1.03 | 7.8 | 30 |
| A9 | 7.83 | 1.73 | 7.5 | 50 | C2 | 3.03 | 0.91 | 7.8 | 20 |
| A10 | 5.58 | 1.08 | 7.9 | 50 | | | | | |
| A11 | 2.95 | 0.8 | 7.1 | 20 | | | | | |

3.2 Strong Motion Attenuation

Several studies of strong motion attenuation have been made using data from the region of interest and from other seismically active areas of the world. For our analysis, we are

interested in the attenuation of PGA and spectral intensity (SI). Molas and Yamazaki [3] is one of those studies which have derived attenuation relationships for both PGA and SI based on a large number of data obtained in Japan by reliable devices. The formula of strong motion attenuation is stated as:

$$\log y = b_0 + b_1M + b_2r + b_3 \log r + b_4h + c_i \pm \sigma p \tag{2}$$

where, y is the intensity measure (either PGA or SI), M is magnitude of an earthquake, r is hypocentral distance, h is hypocentral depth (km), b_0, b_1, b_2, b_3 and b_4 are regression coefficients, c_i is a constant of locality, σ is the standard deviation of regression errors and p is a parameter to represent confidence interval of the estimate. Table 2 shows the values of these coefficients.

Table 2:Coefficients of Strong Motion Attenuation

| y | b_0 | b_1 | b_2 | b_3 | b_4 | c_i | σ |
|-------------------------|-------|-------|----------|-------|---------|-------|----------|
| PGA(cm/s ²) | 0.206 | 0.477 | -0.00144 | -1.00 | 0.00311 | 0.225 | 0.276 |
| SI(cm/s) | -1.64 | 0.614 | -0.00133 | -1.00 | 0.00233 | 0.184 | 0.257 |

3.3 Alternative SEWSs

To find the optimal trade-off between gain in safety and costs associated with false alarms, we consider the following alternatives of SEWS configuration and evaluate their effectiveness.

System A This system is a baseline in comparison with which we examine the effectiveness of other alternative systems. System A is modeled as a warning system which is composed of only the wayside part of the current SEWS. This system operates on S waves and triggers automatic braking for trains on a operational track segment when PGA recorded by the corresponding wayside accelerometer exceeds a threshold value, which is set at 40gals.

System B This system is the system that had been in operation until 1999. It assigns a specific track segment to each of 11 coastal accelerometers in addition to the wayside system configuration of system A. These 11 preset sections, hereafter referred as "shut-down" sections, cover the entire line with some overlap. Each shut-down section is composed of neighboring operational track segments. The controlling policy of the coastal warning of this system is that when the earthquake motion at a coastal accelerometer exceeds a preset intensity, then automatic braking is issued for all trains in the corresponding shut-down section. This system operates on S waves and the threshold value of PGA for triggering automatic braking is set at 40gals for both wayside and coastal accelerometers.

System C The underlying idea of system C is that it should be able to issue warnings with increased lead time for emergency braking if the system can operate on P waves in addition to S waves and also it is able to trigger automatic braking also outside its designated proximal track section when one of the coastal accelerometers detects high ground motion levels that justify ordering of such warnings. In this system, it is the estimated magnitude of the earthquake M and the epicentral location x that determine the area of the track section to be shutdown. A system like this is the UrEDAS: see Nakamura[4]. The UrEDAS evaluates the destructive potential at all locations s along the track based on the estimation of M and x of the earthquake and historical data on damage and non-damage events depending on M and epicentral distance $\Delta(x,s)$. Emergency braking may or may not be ordered depending on the first estimate of M and x from a single station using P waves and the procedure is then repeated using S waves with increased accuracy of the estimation.

System D This system corresponds to the system that is currently in operation on the Tohoku Shinkansen. This system maintains the geographic configuration of the coastal accelerometers and controlling policy of system B, but its coastal system operates on not only S waves but also P waves as in system C. The current system on the Tohoku Shinkansen is called the "Compact" UrEDAS as it is a truncated version of the UrEDAS. Although the details of the method to evaluate the destructive potential of the earthquake used in the Compact UrEDAS are different from those in the UrEDAS, we

regard them as identical in this study for simplicity. In addition to the above-mentioned different system configurations of SEWS, we examine the effect of changing earthquake intensity parameters at wayside stations from PGA to SI, for there is ample engineering evidence that, SI, which takes response spectra of structures into consideration, is far better as a measure of the destructiveness of earthquake motion than PGA.

3.4 Occurrence Rate of Risk Events

In order to avoid derailments, the present SEWS tends to stop trains at a high rate. In a few cases such actions may indeed result in derailment avoidance, but in most cases they produce "false alarms" and unnecessary delays of various durations. Hence, a reasonable way to characterize the performance of the SEWS is to calculate the rate of derailments that were not prevented and the rate of delays of various magnitudes, more specifically, we define four rates:

- $\mu(D)$:annual rate of earthquake-induced *derailments*. This is the expected number of trains per year that derail due to earthquakes, anywhere along the line.
- $\mu(S)$:annual rate of earthquake-induced *short delays*. This is the expected number of trains per year that, after being stopped by the SEWS, are immediately allowed to resume operation without any inspection of the tracks.
- $\mu(M)$:annual rate of earthquake-induced *medium delays*. This is the expected number of trains per year that, after being stopped by the SEWS, resume operation at low speed to perform on board inspection of the track.
- $\mu(L)$:annual rate of earthquake-induced *long delays*. This is the expected number of trains per year that, after being stopped by the SEWS, are not allowed to resume operation until on-foot inspection of the tracks has been completed.

The general procedure to calculate the rates of the events \mathcal{E} of interest (\mathcal{E} can be D, S, M, L , where the symbols stand for derailment, short delay, medium delay, and long delay events) under the given warning system W (W can be A, B, C, D , where the symbols stand for System A, B, C and D) $\mu(\mathcal{E}|W)$ is given by:

$$\mu(\mathcal{E}|W) = \int_M \int_x \sum_s \lambda(M, x) E(n_s) P(\mathcal{E}|M, x, s, W) dx dM \quad (3)$$

where,

- $\lambda(M, x)$ is the rate density per year of earthquakes of magnitude M at epicentral location x . This density is given by Equation (1).
- $E(n_s)$ is the expected number of trains running at a random point in time in operational segment s .
- $P(\mathcal{E}|M, x, s, W)$ is the probability of event \mathcal{E} occurring under the given SEWS for a train running in operational segment s , an earthquake of magnitude M and epicentral location x . This probability may in turn be written as:

$$P(\mathcal{E}|M, x, s, W) = \sum_T P(\mathcal{E}|M, x, s, T) P(T|M, x, s, W) \quad (4)$$

where T is the generic trigger/no-trigger status of SEWS. T has the following logical values: $T=T_c$ for automatic braking triggered by coastal system, $T=T_w$ for automatic braking triggered by wayside system, and $T=T_o$ in the case of no trigger.

4. RISK ANALYSIS

Here we show how the probabilities of various events in the right hand side of Equation (4) are evaluated for different \mathcal{E}, T and W .

4.1 Conditional Probability of Trigger, $P(T|M, x, s, W)$

4.1.1 System A

For System A, there is one-on-one correspondence between an operational track segment and a wayside accelerometer and no coastal system is installed. Therefore, automatic emergency braking occurs for an operational track segment when the intensity of the earthquake recorded at the designated wayside accelerometer exceeds the preset threshold value. Trigger probability for system A is obtained as:

$$P(T_w|M, x, s, A) = P(y_w(M, r(x, s)) \geq Y_w^*) \tag{5}$$

where, $r(x, s)$ is the distance between x and s and $y_w(M, r(x, s))$ is the attenuated intensity of an earthquake of magnitude M at the operational track segment s and Y_w^* is the trigger threshold for a wayside accelerometer.

4.1.2 System B

For system B, if either of designated coastal and wayside accelerometers record the levels of the earthquake intensity that exceed the preset threshold value, it is the one that is the closest of all to the epicenter which issues emergency braking. The probability of coastal trigger T_c is given as:

$$P(T_c|M, x, s, B) = \begin{cases} P(y_c(M, r(x, i)) \geq Y_c^*); (r(x, s) \geq r(x, i)) \\ (1 - P(y_w(M, r(x, s)) \geq Y_w^*))P(y_c(M, r(x, i)) \geq Y_c^*); (r(x, s) < r(x, i)) \end{cases} \tag{6}$$

where, $y_c(M, r(x, i))$ is the attenuated intensity of an earthquake of magnitude M at coastal station i and Y_c^* is the trigger threshold for a coastal accelerometer. The probability of wayside trigger T_w is given as:

$$P(T_w|M, x, s, B) = \begin{cases} P(y_w(M, r(x, s)) \geq Y_w^*); (r(x, s) < r(x, i)) \\ (1 - P(y_c(M, r(x, i)) \geq Y_c^*))P(y_w(M, r(x, s)) \geq Y_w^*); (r(x, s) \geq r(x, i)) \end{cases} \tag{7}$$

And the probability of no-trigger T_0 is given as:

$$P(T_0|M, x, s, B) = (1 - P(y_c(M, r(x, i)) \geq Y_c^*)) (1 - P(y_w(M, r(x, s)) \geq Y_w^*)) \tag{8}$$

4.1.3 System C

System C may trigger upon the arrival of either P or S waves to the coastal stations. For given estimates of M and Δ , the system causes trains to stop if the parameter y given as below is larger than the preset threshold value Y .

$$y = 0.71\hat{M} - \log_{10}\hat{\Delta}(x, i) \tag{9}$$

where, $M, \Delta(x, i)$ are estimated magnitude and epicentral distance by the UrEDAS. Considering uncertainty on the estimates of (M, x) , y may be modeled as a random variable with normal distribution, mean value given by Equation (9) and variance,

$$\sigma_u^2 = (0.71\sigma_M)^2 + \left(\log \frac{\sigma_\Delta}{\Delta}\right)^2 \tag{10}$$

Based on the data about empirical performance of the UrEDAS, we consider the following as reasonable values for the standard deviation of the estimation error for earthquake magnitude and epicentral distance from P wave arrival and those from S wave arrival.

$$\sigma_{M,p} = 1.0 \quad \sigma_{\Delta,p} = 0.5\Delta \tag{11}$$

$$\sigma_{M,s} = 0.5 \quad \sigma_{\Delta,s} = 0.25\Delta \tag{12}$$

For system C, the probability that a coastal station triggers on the arrival of P waves is given as:

$$P(T_{c,p}|M, x, s, C) = P(y_p \geq Y^*) \tag{13}$$

and the probability that a coastal station triggers on the arrival of S waves is given as:

$$P(T_{c,s}|M, x, s, C) = (1 - P(y_p \geq Y^*))P(y_s \geq Y^*) \tag{14}$$

where y_p and y_s are estimated value of y based on P waves and S waves, respectively. Also, the probability of no-trigger at a coastal station is given as:

$$P(T_{0,c}|M, x, s, C) = (1 - P(y_p \geq Y^*)) (1 - P(y_s \geq Y^*)) \tag{15}$$

Considering that each track segment along the line can be triggered by all coastal stations in the case of system C, the probability that k -th ($k = 1, 2, \dots$) arrival of P or S waves to any of coastal stations triggers the emergency braking of trains along the track segment s is given as:

$$P(T_k|M, x, s, C) = P(y(k, x, M) \geq Y^*(k, s)) \prod_{i=1}^{k-1} (1 - P(y(i, x, M) \geq Y^*(i, s))) \tag{16}$$

4.1.4 System D

For system D, which is a truncated version of system C, the probabilities of various T are given also by equation (6),(7) and (8).

4.2 Seismic Fragility of the Viaduct Structure

A key component of the seismic risk analysis is the evaluation of the probability of the viaduct damage in an operational segment s under the given ground motion intensity. Fragility curves are estimated by Yamaguchi and Yamazaki [5] for generic reinforced concrete buildings using both PGA and SI based on the data from the Kobe earthquake as:

$$P_d(y) = \Phi\left(\frac{\ln y - \lambda}{\zeta}\right) \tag{17}$$

where, $P_d(y)$ is the probability that a building being damaged at by an earthquake of intensity y , Φ is the symbol for probability distribution function of the standard normal density, λ is the mean and ζ is the variance. The parameters of Equation(17) is estimated as Table 3.

Table 3: Parameters of the Fragility Curve for Generic RC Buildings

| y | λ | ζ |
|-------------------------|-----------|---------|
| PGA(cm/s ²) | 7.34 | 0.912 |
| SI(cm/s) | 5.31 | 0.844 |

The viaduct structure of the Tohoku Shinkansen is composed of a series of short spans with length $SP = 7m$. Assuming the number of continuously damage or continuously undamaged spans of the viaduct has a geometric (essentially exponential) distribution, the relation between the mean number of continuously undamaged spans $n_0(y)$ and the probability $P_1(y)$ that a single viaduct span is damaged, given that the local level of earthquake intensity is y as follows:

$$n_0(y) = \frac{1 - P_d(y)}{P_d(y)} \tag{18}$$

4.3 Probability of Derailment

We assume that the intensity of an earthquake at the track reaches its maximum value instantly and that a train of length L travels a distance LE after the arrival of the S waves. We define the probability of derailment P_d as the probability that the train meets damaged track

(note that derailment due to vibratory motion without structural damage is excluded). Under these simplifying assumptions, the event of no-derailment occurs only if the last point of the train, coming from undamaged conditions (before the strong vibratory motion arrives at the track), encounter no damage in track length LE and stops instantly, and if the instant before stopping, the section of track of length L occupied by the train is entirely undamaged given that it is undamaged at the location where the train terminates. From the fact that the distribution of undamaged and damaged section is exponential and using Equation (17), the probability of no-derailment given y is given by:

$$P(n_0 D | y) = e^{-[(LE+L)(SP)]/n_0(y)} \tag{19}$$

Therefore, taking complimentary probability, the probability of derailment is given as:

$$P(D | y) = 1 - P(n_0 D | y) = 1 - e^{-[(LE+L)(SP)]/n_0(y)} \tag{20}$$

Taking the expectation of Equation (20), the probability of derailment, $P_d(M, x, s)$ of a train running is operational segment s , given the occurrence of an earthquake of magnitude M at epicentral location x is given by:

$$P(D | M, x, s) = 1 - E_{y|M, x, s} [e^{-[(LE+L)(SP)]/n_0(y)}] \tag{21}$$

In Equation(21), LE is the length of track that a train in operational segment s covers and has the following values depending on whether or not of the occurrence of emergency braking from the coastal station. When emergency braking is ordered, LE is equal to $D_{stop} = \{v_0^2\}/2a_e$, where v_0 is the speed of the train when braking starts and a_e is the deceleration of the emergency braking. If not for the occurrence of emergency braking, LE is equal to $SEC(s)$, the half of the average distance between trains in s in the same direction. Therefore,

$$P(D | M, x, s, T_{c,w}) = (1 - E_{y|M, x, s} [e^{-[(D_{imp}+L)(SP)]/n_0(y)}]) \tag{22}$$

$$P(D | M, x, s, T_0) = (1 - E_{y|M, x, s} [e^{-[(SEC(s)+L)(SP)]/n_0(y)}]) \tag{23}$$

4.4 Probability of Various Delays

Delays can be caused by either the coastal or the wayside system; these events are denoted by T_c and T_w as indicated earlier. Here we give formulas for just the former, for the reasons of brevity. The equations are completely analogous for an T_w based operation.

$$P(S | M, x, s, W) = P[y(M, \Delta(x, s)) \leq Y_{insp1}] \tag{24}$$

$$P(M | M, x, s, W) = P[Y_{insp1} \leq y(M, \Delta(x, s)) \leq Y_{insp2}] \tag{25}$$

$$P(L | M, x, s, W) = P[Y_{insp2} \leq y(M, \Delta(x, s))] \tag{26}$$

where, Y_{insp1} and Y_{insp2} are the threshold intensity for on board inspection and on foot inspection, respectively.

5. RISK RESULTS

We calculated the rate of the four risk events: derailment $\mu(D)$, short delay $\mu(S)$, medium delay $\mu(M)$ and long delay $\mu(L)$ for the four SEWS configurations: system A, system B, system C, system D and a modified system D, in which SI is chosen as the wayside intensity parameter instead of PGA. We calculated Equation (3) with the setting of M at the interval of 0.1 and x into 194 discrete point sources. The results of the comparison between four alternative in terms of the rate of events are given in Table 4. Our main findings on the effectiveness of these systems are as follows:

Table 4: Risk Results

| | $\mu(D)$ | $\mu(S)$ | $\mu(M)$ | $\mu(L)$ |
|--------------|----------|----------|----------|----------|
| System A | 0.062 | 2.304 | 0.636 | 0.284 |
| System B | 0.059 | 7.850 | 0.646 | 0.284 |
| System C | 0.056 | 45.066 | 0.646 | 0.284 |
| System D | 0.058 | 22.927 | 0.646 | 0.284 |
| System D(SI) | 0.058 | 21.870 | 0.232 | 0.117 |

Coastal station The reduction of $\mu(D)$ caused by coastal stations in system B compared with system A, which has no coastal stations, is by about 5%. The coastal system has no effect on the rates of medium and long delays, which are controlled by the wayside system. On the other hand, the coastal system is the primary cause of false alarms, whose rate depends on the level of ground motion at which trains are stopped.

P wave detection The additional reduction of $\mu(D)$ caused by coastal stations in system D, which can operate on P waves, compared with system B, which operates only on S waves, is disappointingly small. On the other hand, it causes about three times as many short delays as the coastal system B does in its original setting $Y_c^* = Y_w^* = 40$ gals.

Triggering policy The additional reduction of $\mu(D)$ caused by coastal stations in system C, in which any of the coastal accelerometer can order emergency braking of trains anywhere along the track, compared with system D, in which emergency braking is ordered only to the designated shut-down section of a coastal accelerometer, is also very modest. On the other hand, it causes about twice as many short delays as the coastal system D does.

Alternative measures of seismic intensity there is a great advantage in changing the intensity parameter of the wayside system of the current SEWS from PGA to SI. As is designated as system D(SI) in Table 4, it can reduce the rate of long and medium delays at least in half without increasing the rate of derailments.

6. CONCLUSIONS

The effectiveness of various configurations of SEWS for the Tohoku Shinkansen was discussed in this paper. As the result of quantitative risk analysis, we found, most importantly, warning efficiency of the SEWS will be significantly improved if the earthquake intensity parameter at the wayside stations is changed from PGA to SI irrespective to the coastal system that is finally chosen.

7. REFERENCES

- [1] A. Papadimitriou and D. Veneziano. (1995) Seismic Safety of the Tohoku Shinkansen: Assessment and Enhancement, Thesis-Related report, Massachusetts Institute of Technology, August 1995.
- [2] M. Shimamura, M. Horiuchi and H. Fukuyama. (1997) A Macroscopic Risk Assessment Method for Railway Systems, IATSS Research vol.21, No.2, 1997
- [3] G. L. Molas and F. Yamazaki. (1995) Attenuation of Earthquake Ground Motion in Japan Including Deep Focus Events, Bulletin of the Seismological Society of America, 85, 5, pp. 1343-1358, 1995. 10
- [4] Y. Nakamura. (1999) On the UrEDAS-its Development and Application for early Warning and Rapid Information against destructive Earthquakes, Proceedings of the first U.S.-Japan Workshop on Seismic Information systems, November 1999
- [5] N. Yamaguchi and F. Yamazaki. (2000) Fragility Curves for Buildings in Japan based on Damage Surveys after the 1995 Kobe Earthquake, 12th World Conference on Earthquake Engineering, CD-ROM, 8p, January 2000